

Cosmological test on viscous bulk models using Hubble Parameter measurements and type Ia Supernovae data

A. Hernandez-Almada^{1*}

¹*Facultad de Ingeniería, Universidad Autónoma de Querétaro,
Centro Universitario Cerro de las Campanas, 76010, Santiago de Querétaro, México*
(Dated: October 4, 2022)

From a phenomenological point of view, we analyze the dynamics of the Universe at late times by introducing a polynomial and hyperbolic bulk viscosity into the Einstein field equations respectively. We constraint their free parameters using the observational Hubble parameter data and the Type Ia Supernovae dataset to reconstruct the deceleration q and the jerk j parameters within the redshift region $0 < z < 2.5$. At current epochs, we obtain $q_0 = -0.780^{+0.070}_{-0.064}$ and $j_0 = 4.057^{+0.851}_{-0.922}$ for the polynomial model and $q_0 = -0.557^{+0.020}_{-0.020}$ ($-0.648^{+0.038}_{-0.042}$) and $j_0 = 0.329^{+0.031}_{-0.031}$ ($1.378^{+0.190}_{-0.166}$) for the tanh (cosh) model. Furthermore we explore the statefinder diagnostic that give us evident differences with respect to the concordance model (LCDM). According to our results this kind of models is an interesting alternative to LCDM to understand the nature and dynamics of the Universe in the context of unified dark fluids.

Keywords: Cosmology, Viscous bulk

I. INTRODUCTION

Currently the Universe is into an accelerated expansion phase supported by several cosmological observations coming from type Ia supernovae (SNIa) [1, 2], the large-scale structure (LSS) [3], cosmic microwave background radiation (CMB) [4, 5], baryon acoustic oscillations (BAO) [6]. Together with the observations coming from spiral galaxies [7, 8] and galaxy clusters [9], the Universe contains more matter than the observed one known as dark matter (DM), and is responsible of the structure formation. The simplest cosmological model called Λ -Cold Dark Matter (LCDM) describes these phenomena as two components that constitute the dark sector and is estimated to be about 95% of the Universe. The accelerated expansion is well described by a cosmological constant (CC) with equation of state (EoS) $p = -\rho$, and the structure formation is due by dust matter ($p = 0$). Despite its good agreement to cosmological observations, LCDM presents several problems at galactic scales and open questions about the CC origin. Therefore, alternative models have been emerging to solve the LCDM inconsistencies. To explain the DM, we have axions [10, 11] (and ref. therein), ultralight scalar particles [12–17], supersymmetry particles [18], and among others. However, the cosmic measurements are not able to determine if the dark sector is constituted by two dark components due the gravity theories only estimate the total energy-momentum tensor. This is known as *the degeneracy problem* [19, 20].

Motivated by this problem, a plenty of models proposes to explain the dark sector as an unique component or fluid that behaves as DM at high redshift and as DE at low redshift to model the current acceleration of the

Universe solving the degeneracy problem. Between them we have the (Generalized) Chaplygin gas [21–25] with EoS ($p = A/\rho^n$) $p = A/\rho$ where A and n are constants, logotropic dark fluid [26] with $p = A \log(\rho/\rho_p)$ where ρ_p is the Planck constant. More recently has been appearing models that generalize the perfect fluids EoS as $p = -\rho + \rho \text{sinc}(\rho_0/\rho)$ where ρ_0 is the energy density at current epochs [27, 28]. It is interesting to see that these models propose alternatives to the CC EoS. On the other hands, an interesting mechanism of unifying DM and DE supposes a Universe filled with a viscous fluid instead of a perfect fluid [29, 30]. In this framework the accelerated expansion of the Universe is due to viscous fluid pressure instead of a CC. Thus this kind of Unified DM models also avoids CC problems, such as the *the cosmological constant problem* and *coincidence problem* [31, 32]. Moreover, by taking into account viscous fluids, it is possible to avoid singularities at the future, called Big Rips [33], that appears when the DE models are in the phantom region, *i.e.*, $p/\rho < -1$ [34]. In this context, there are mainly two approaches to address the bulk viscosity, the Eckart [35] and the Israel-Stewart-Hiscock (ISH) [36], and both have advantages and disadvantages. For instance, besides the ISH approach solves the problem of the causality, *e.i.*, the perturbations are propagated with a finite speed, it is more complex than the Eckart's one that only are known some analytical solutions when the viscosity is assumed in the form $\xi = \xi_0 \rho^s$; in particular the case $s = 1/2$, see for instance [37–40]. An inconvenient of this form is that ξ diverges at high densities or early epochs of the Universe. Regarding the Eckart's formalism, it is the simplest one but is a non-causal theory where the perturbations in the viscous fluid are moved at infinite speed; however, there are proposals that solve this problem by including correction terms of $\mathcal{O}(1/c^2)$ in the theory (see [41] for more details). Only some polynomial models of the bulk viscosity have been studied

* ahalmada@uaq.mx

widely [42–44]. Hence, we motivate this work to explore more complex functions of the bulk viscosity in the Eckert approach.

In this work we aim to revisit three viscous fluid models and constraint their free parameters by performing a Bayesian Markov Chain Monte Carlo (MCMC) analysis with the latest cosmological data of the Hubble parameter (OHD) and SNIa distances at the background level. We use the OHD and SNIa measurements collected by [45] and [46] respectively. The first viscous model consists of a Universe with a polynomial bulk viscosity as function of the redshift proposed by [44]. This model is built as a generalized form of the constant bulk viscosity studied in [47]. The second model contains a more complex form for the bulk viscosity that involves the tanh function that depends of the Hubble parameter E and was proposed by [48]. Finally, as alternative to tanh form we explore the Universe dynamics by proposing a cosh form for the bulk viscosity. The last one is motivated by the fact that cosh function has been used widely as scalar potentials to study the dark sector. Then in our case we will use to model the bulk viscosity. In these models the bulk viscosity terms are introduced into Einstein field equations as an effective pressure and following the Eckert' approach [35].

This paper is structured as follows. In Sec. II, we present the generals on the viscous fluid models under study. Section III describes the OHD and SNIa sample to constraint the viscous fluid models and we also explain the configuration for the Bayesian statistical analysis. In Sec. IV we give a discussion. Finally, in Sec. V we present the conclusions of our results.

II. FLUID VISCOUS MODEL

We study the dynamics of the Universe considering a flat Friedmann-Roberson-Walker (FRW) metric, *i.e.* $ds^2 = -dt^2 + a(t)(dr^2 + r^2 d\Omega^2)$, where a is the scale factor and t is the cosmic time containing a viscous fluid. Thus we introduce the bulk viscosity Π component as a pressure term into the energy-momentum tensor,

$$T_{\mu\nu} = \rho U_\mu U_\nu + (p + \Pi)(g_{\mu\nu} + U_\mu U_\nu). \quad (1)$$

where $U^\mu = (1, 0, 0, 0)$ in the co-moving coordinates. From the Einstein field equations, the Friedmann equations are

$$H^2 = \frac{\kappa^2}{3} \rho, \quad (2)$$

$$\dot{H} + H^2 = \frac{2}{3}(\rho + 3\tilde{p}), \quad (3)$$

where $H = \dot{a}/a$ is the Hubble parameter, $\tilde{p} = p + \Pi$ is the effective pressure and $\Pi = -3\xi H$, with ξ the bulk viscosity. Then the continuity equation is given by

$$\dot{\rho} + 3H\rho = 3\xi H. \quad (4)$$

We define the dimensionless Hubble parameter as

$$E(t)^2 = \frac{H(t)^2}{H_0^2} = \frac{\rho}{\rho_{cr}}, \quad (5)$$

where ρ_{cr} is the critical density. From Eqs. (2), (3), (5) and the relation $z = 1/a - 1$ we obtain

$$-2(1+z)\frac{dE}{dz} + 3E = 9\lambda, \quad (6)$$

where we have defined $\lambda = \xi H_0 / \rho_{cr}$. It is interesting to notice that the Eq. (6) gives a linear correlation between deceleration parameter $q(z)$ and the dimensionless bulk viscosity $\lambda(z)$, we can study this kind of models by proposing phenomenological functions to describe the parameter q at late times. Hence, from Eq. (6) we can write the deceleration parameter as

$$q(z) = \frac{1}{2} - \frac{1}{2E(z)} 9\lambda(z). \quad (7)$$

Notice that it is interesting that this expression allows to propose a phenomenological behaviour of $\lambda(z)$ to model the accelerated dynamics of the Universe.

We also analyze the statefinder (SF) diagnostic that is useful to distinguish the behaviour of different cosmological models of LCDM model. The SF diagnostic is a $\{s, r\}$ -plane defined by the geometric variables [49, 50]

$$r = j = \frac{\ddot{a}}{aH^3}, \quad (8)$$

$$s = \frac{r - 1}{3(q - 1/2)}, \quad (9)$$

where r is the jerk parameter and q is the deceleration one. In this phasespace, LCDM is a fixed point located at $(s, r) = (0, 1)$, the trajectories in the region $r < 1$ and $s > 0$ corresponds to quintessence behaviour and trajectories in the region $r < 1$ and $s < 0$ presents a GC one.

The jerk parameter can be expressed in terms of $q(z)$ and its first derivative with respect to z as [51]

$$j(q) = q(2q + 1) + (1 + z)\frac{dq}{dz}. \quad (10)$$

For LCDM model the jerk parameter is $j = 1$ that we will be used to compare with our models.

A. Polynomial function

We consider the polynomial function of λ given by [44]

$$9\lambda(z) = \lambda_0 + \lambda_1(1+z)^n, \quad (11)$$

where λ_0 , λ_1 , and n are free parameters to be determined by data sets. The simplest case, $\lambda = \text{constant}$, was studied in [42]. Substituting Eq. (11) in Eq. (6), we obtain the solution

$$E(z) = \lambda_2(1+z)^{3/2} - \frac{\lambda_1}{2n-3}(1+z)^n + \frac{\lambda_0}{3}, \quad (12)$$

where

$$\lambda_2 = 1 + \frac{\lambda_1}{2n-3} - \frac{\lambda_0}{3}. \quad (13)$$

The deceleration parameter is given by

$$q(z) = -1 + \frac{\frac{3}{2}\lambda_2(2n-3)(z+1)^{3/2} - \lambda_1 n(z+1)^n}{\frac{1}{3}\lambda_0(2n-3) + \lambda_2(2n-3)(z+1)^{3/2} - \lambda_1(z+1)^n}. \quad (14)$$

Notice that for $n < 0$, $q(z) \rightarrow 1/2$ when $z \rightarrow \infty$. The jerk parameter can be expressed as

$$j(z) = 1 + \frac{1}{E^2} \left(\frac{1}{2}\lambda_0^2 + \lambda_0\lambda_1(z+1)^n + \frac{1}{2}\lambda_1^2(z+1)^{2n} - \frac{3}{2}\lambda_0 E - \frac{1}{2}\lambda_1(n+3)(z+1)^n E + \frac{1}{2}\lambda_0(z+1)\frac{dE}{dz} + \frac{1}{2}\lambda_1(z+1)^{n+1}\frac{dE}{dz} \right), \quad (15)$$

where

$$\frac{dE}{dz} = \frac{3}{2}\lambda_2(z+1)^{1/2} - \frac{n}{2n-3}\lambda_1(z+1)^{n-1}. \quad (16)$$

Notice that the jerk parameter for LCDM model is $j = 1$.

B. Hyperbolic function

Motivated for describing the evolution of the Universe from recombination to late acceleration phase, the authors [48] proposed the hyperbolic behavior of λ given by

$$9\lambda(z) = 3 \tanh\left(\frac{b}{E(z)^n}\right), \quad (17)$$

where b and n are free parameters that we will determine by the cosmological data set. The jerk parameter is expressed as

$$j(z) = 1 + \frac{9}{4}bnE^{-n-1} - \left(\frac{9}{4}bnE^{-n-2} + \frac{9}{4}E^{-1}\right)\tanh(bE^{-n}) - \left(\frac{9}{4}bnE^{-n-1} - \frac{9}{4}E^{-2}\right)\tanh^2(bE^{-n}) + \frac{9}{4}bnE^{-n-2}\tanh^3(bE^{-n}), \quad (18)$$

where $E(z)$ will be obtained by solving differential equation numerically.

As alternative model to (17), we study the phenomenological bulk viscosity model expressed as

$$9\lambda(z) = \cosh\left(\frac{b}{E(z)^n}\right). \quad (19)$$

TABLE I: Priors considered for the polynomial (top panel) and hyperbolic (bottom panel) models. The priors for the polynomial model are based on [44].

Parameter	Prior
Polynomial model	
λ_0	Flat in $[0, 2]$
λ_1	Flat in $[0, 4]$
n	Flat in $[-5, 0]$
h	Gauss(0.7324, 0.0174)
tanh/cosh model	
b	Flat in $[0, 3]$
n	Flat in $[0, 5]$
h	Gauss(0.7324, 0.0174)

The deceleration parameter is straightforward obtained from Eq. (7) and the jerk parameter can be expressed as

$$j(z) = 1 + \frac{1}{8}E^{-2} + \frac{3}{4}bnE^{-n-1}\sinh(bE^{-n}) - \frac{1}{8}bnE^{-n-2}\sinh(2bE^{-n}) - \frac{3}{4}E^{-1}\cosh(bE^{-n}) + \frac{1}{8}E^{-2}\cosh(2bE^{-n}). \quad (20)$$

Again, for LCDM model we have $j = 1$. The next section is devoted to describe the cosmological data used in this work.

III. COSMOLOGICAL DATA

In this section we describe the observational datasets used to perform the confidence region of the free model parameters. We perform a Bayesian Chain Markov Monte Carlo analysis based on emcee module [52] by setting 5000 chains with 500 steps. The nburn is stopped up to obtain a value of 1.1 on each free parameters in the Gelman-Rubin criteria [53]. We search the confidence region according on the priors presented in Table I and using the Hubble parameter measurements and supernovae data. To compare the hyperbolic models with the data, we implement a second order Runge-Kutta procedure to solve the corresponding ODE with the functions given in Eqs. (17) and (19) respectively. For the polynomial viscous model we use the exact solution of $E(z)$ given in Eq. (12).

We perform a joint analysis by combining the OHD and SNIa data through the merit-of-function

$$\chi_{joint}^2 = \chi_{OHD}^2 + \chi_{SNIa}^2, \quad (21)$$

where χ_{OHD}^2 and χ_{SNIa}^2 refer to the chi-square. The rest of the section is devoted to describe the observational data and the construction of each χ^2 functions.

A. Hubble Parameter Data

The Universe is in a expansion rate that is measured through the Hubble parameter measurements (OHD) and are cosmological-model independent measurements. The OHD give are measurements of the Hubble parameter, $H(z)$, as a function of the redshift z and the latest ones are obtained by the differential age (DA) tool [54] and BAO measurements. We consider the OHD compilation provided by [45] that consists of 51 data points within the redshift region $[0, 2.36]$. Thus we constraint the free parameters of the viscous models by building the chi-square as

$$\chi_{OHD}^2 = \sum_i^{51} \left(\frac{H_{th}(z_i) - H_{obs}}{\sigma_{obs}^i} \right)^2 \quad (22)$$

where the $H_{th}(z_i)$ and $H_{obs}(z_i) \pm \sigma_{obs}^i$ are the theoretical and observational Hubble parameter at the redshift z_i respectively.

B. Type Ia Supernovae

The Pantheon compilation given by [46] contains the observations of the luminosity modulus coming from 1048 type Ia supernovae (SNIa) located in the region $0.01 < z < 2.3$. For simplicity we do not consider the correlation between points of the SNIa sample and only will consider the diagonal components of the covariance matrix provided in [46], then we obtain the free parameters of the models by minimizing the expression

$$\chi_{SNIa}^2 = A - B^2/C \quad (23)$$

where

$$\begin{aligned} A &= \sum_i^{1048} \left(\frac{m_{th}(z_i) - m_{obs}}{\sigma_{m_{obs}}} \right)^2, \\ B &= \sum_i^{1048} \left(\frac{m_{th}(z_i) - m_{obs}}{\sigma_{m_{obs}}^2} \right), \\ C &= \sum_i^{1048} \frac{1}{\sigma_{m_{obs}}^2}. \end{aligned} \quad (24)$$

where $m_{obs} \pm \sigma_{m_{obs}}$ is the observational bolometric apparent magnitude and its uncertainty at the redshift z_i and is related with the distance modulus μ by $m = \mu + M$, where M the absolute bolometric magnitud. The theoretical one, $m_{th}(z_i)$, is estimated by

$$m_{th}(z) = \mathcal{M} + 5 \log_{10} [d_L(z)/10 pc]. \quad (25)$$

Here, \mathcal{M} is a nuisance parameter and $d_L(z)$ is the dimensionless luminosity distance

$$d_L(z) = (1+z)c \int_0^z \frac{dz'}{H(z')} \quad (26)$$

where c is the speed of light. Notice that the form of χ_{SNIa}^2 in Eq. (23) allows to marginalize over the nuisance parameter \mathcal{M} .

IV. DISCUSSIONS

The best fit values of free model parameters obtained by our OHD, SNIa and joint analysis are summarized in the Tab. II for the polynomial model and in the Tab. III for the hyperbolic models. The uncertainties showed correspond at 68% (1σ) confidence Level (CL). Also, we present the $1\sigma, 2\sigma, 3\sigma$ CL 2D contours and 1D marginalized posterior distributions of the model parameters in Figs. 1, 2, and 3 for polynomial, tanh, and cosh models respectively using OHD, SNIa and joint analysis. From now, we use the best values obtained in the joint analysis for our discussions. For the polynomial model, [44] estimates best fitting yields around $\lambda_0 \approx 0.1$, $\lambda_1 \approx 2.0$ considering the parameter n to be fixed in the fit (for more details see Table 1 of [44]). These values are consistent within 2σ CL when we compare with our results using SNIa data with those obtained in [44]. For tanh model we obtain a yield value of the b parameter consistent within 3σ CL and a deviation of about 4.8σ CL for the parameter n with those reported by [48].

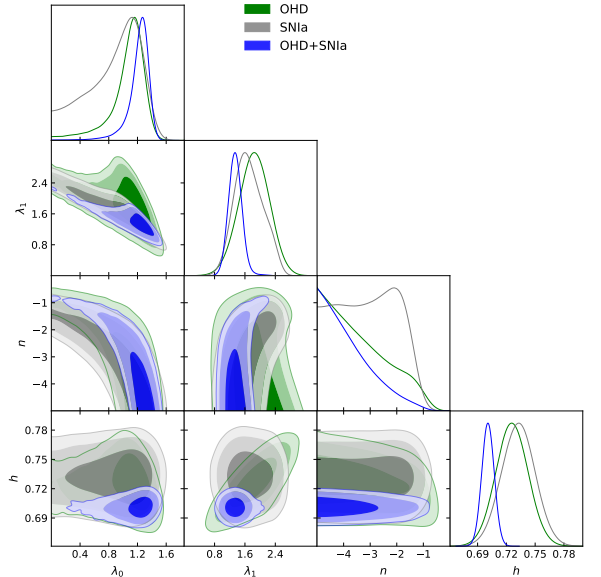


FIG. 1: 68, 97 and 99.7% CL for free model parameters considering $9\lambda = \lambda_0 + \lambda_1(1+z)^n$.

TABLE II: Best fitting parameters of the polynomial model.

Data	χ^2	Polynomial model				
		λ_0	λ_1	n	h	
OHD	12.4	$1.110^{+0.154}_{-0.246}$	$1.840^{+0.400}_{-0.408}$	$-3.630^{+1.530}_{-0.990}$	$0.726^{+0.017}_{-0.017}$	
SN Ia	1032.5	$0.945^{+0.283}_{-0.512}$	$1.680^{+0.441}_{-0.355}$	$-3.050^{+1.200}_{-1.320}$	$0.732^{+0.017}_{-0.018}$	
OHD+SN Ia	1044.9	$1.240^{+0.099}_{-0.145}$	$1.340^{+0.176}_{-0.172}$	$-4.010^{+1.190}_{-0.709}$	$0.701^{+0.006}_{-0.006}$	

TABLE III: Best fitting parameters of the tanh and cosh models.

Hyperbolic models					
tanh model					
Data	χ^2	b	n	h	
OHD	14.1	$0.937^{+0.088}_{-0.087}$	$1.230^{+0.376}_{-0.350}$	$0.713^{+0.014}_{-0.015}$	
SN Ia	1032.1	$1.010^{+0.056}_{-0.053}$	$2.810^{+0.640}_{-0.575}$	$0.732^{+0.017}_{-0.017}$	
OHD+SN Ia	1049.8	$0.876^{+0.028}_{-0.027}$	$1.120^{+0.182}_{-0.174}$	$0.699^{+0.006}_{-0.007}$	
cosh model					
Data	χ^2	b	n	h	
OHD	13.3	$1.580^{+0.084}_{-0.098}$	$1.79^{+0.939}_{-0.605}$	$0.724^{+0.016}_{-0.016}$	
SN Ia	1032.0	$1.530^{+0.047}_{-0.049}$	$2.28^{+0.650}_{-0.553}$	$0.733^{+0.017}_{-0.017}$	
OHD+SN Ia	1046.6	$1.470^{+0.040}_{-0.038}$	$1.46^{+0.390}_{-0.300}$	$0.699^{+0.006}_{-0.006}$	

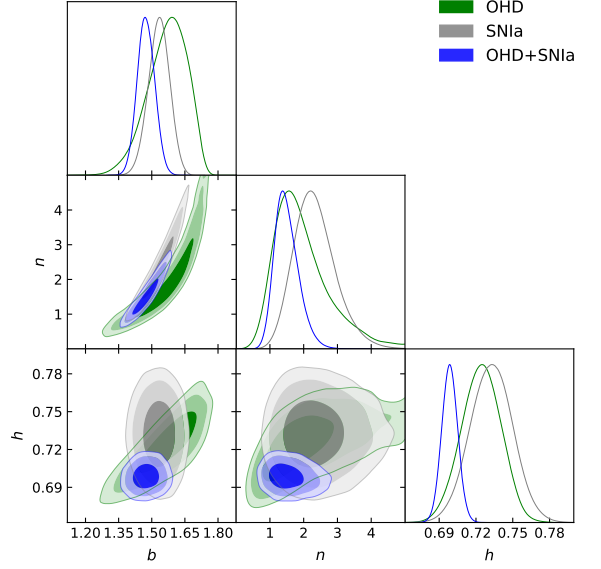
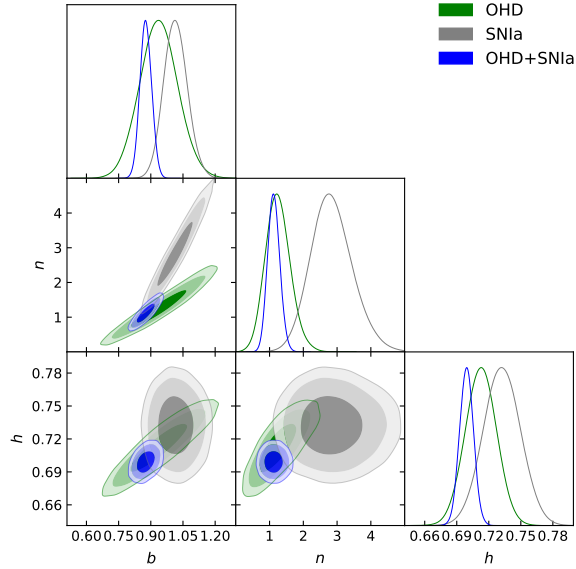
FIG. 3: 68, 97 and 99.7% CL for the free model parameters considering $9\lambda = \cosh(bE(z)^{-n})$.FIG. 2: 68, 97 and 99.7% CL for free model parameters considering $9\lambda = 3 \tanh(bE(z)^{-n})$.

Figure 4 displays the best curves of the models over $H(z)$ data. To compare with LCDM model we also performed a MCMC joint analysis to obtain its best fitting parameters. Taking into account $\Omega_r = 2.469 \times 10^{-5} h^{-2} (1 + 0.2271 N_{eff})$ where $N_{eff} = 3.04$, [55] the best fitting values are $\Omega_{m0} = 0.276^{+0.008}_{-0.008}$ and $h = 0.699^{+0.006}_{-0.006}$.

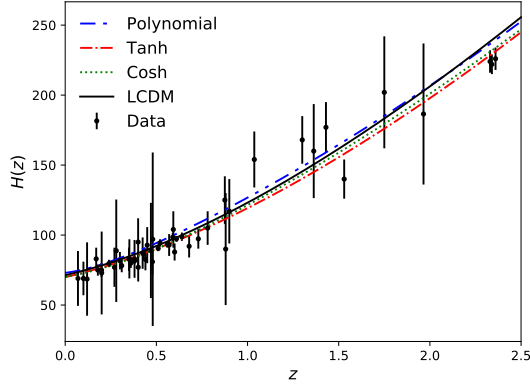


FIG. 4: Best fit curves using the results of the joint analysis for LCDM (black solid line), polynomial (blue double dash-dotted line), tanh (red dash-dotted line), and cosh (green dotted line) models. For LCDM, we use $\Omega_m = 0.276$, and $h = 0.699$. The black points with uncertainty bars correspond to OHD.

Figure 5 shows the reconstruction of the deceleration q (top panel) and jerk j (bottom panel) parameters with respect to the redshift in the region $0 < z < 2.5$. While the polynomial and cosh models present a deceleration-acceleration transition later than the concordance model ($z_t^{LCDM} \approx 0.72$), the tanh model presents such transition earlier. The jerk parameters of the models present the following behavior with respect to LCDM. The jerk parameter for the polynomial model has a lower-bigger transition around $z_t^{jerk} \approx 0.45$ and an increasing trend at current epochs. Similarly, the cosh model has a change from lower to bigger values around $z \approx 0.59$ but has a maximum value less than 1.5 at current epochs. The tanh model presents a jerk values less than 1 for $z < 2.5$.

We estimate the q and j parameter values at current epochs $q_0 = -0.780^{+0.070}_{-0.064}$, $-0.557^{+0.020}_{-0.020}$, $-0.648^{+0.038}_{-0.042}$ and $j_0 = 4.057^{+0.851}_{-0.922}$, $0.329^{+0.031}_{-0.031}$, $1.378^{+0.190}_{-0.166}$ for the polynomial, tanh and cosh models respectively. These q_0 values are consistent up to 99.7% CL with the one obtained for the LCDM model ($q_0^{LCDM} = -0.586^{+0.012}_{-0.011}$). With respect to the current value j_0 , the polynomial and tanh models present a deviation more than within 3σ CL with respect to LCDM one ($j^{LCDM} = 1$). In contrast, the j_0 of the cosh model is consistent to LCDM one within 2.3σ CL.

The Akaike information criterion (AIC) [56, 57] and the Bayesian information criterion (BIC) [58] are useful tools to compare models statistically defined by $AIC = \chi^2 + 2k$ and $BIC = \chi^2 + 2k \ln(N)$ respectively where χ^2 is the chi-square function, k is the number of estimated parameters and N is the number of measurement. In these technique the model preferred by data is the one that has the minimum values on AIC and BIC. Hence taking into account the χ^2 yields values reported in Tab. II and III, we obtain $AIC^{pol,tanh,cosh} = 1052.9, 1055.8, 1052.6$

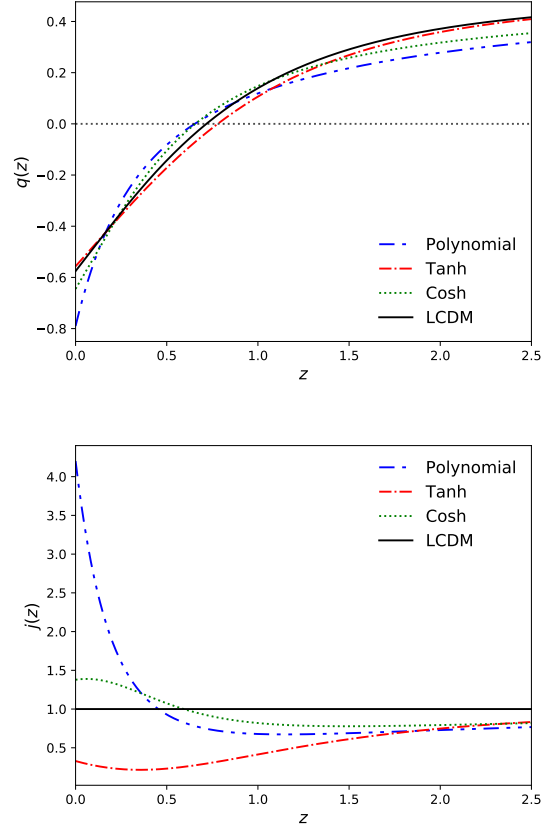


FIG. 5: Reconstruction of the deceleration and jerk parameter using the best fit values of the OHD+SNia analysis for LCDM (black solid line), polynomial (blue double dash-dotted line), tanh (red dash-dotted line), and cosh (green dotted line) models.

and $AIC^{LCDM} = 1086.3$, and $BIC^{pol,tanh,cosh} = 1100.9, 1091.8, 1088.6$ and $BIC^{LCDM} = 1110.3$. Following the convention presented in [59, 60] for these criteria, it is interesting to see that the data (OHD and SNia) prefer a Universe filled with a bulk viscosity than one filled by a perfect fluid (LCDM). Between the phenomenological viscous models, the data prefer equally a Universe filled with a bulk viscosity modeled by a hyperbolic or a polynomial behaviour. Although the polynomial model is a simpler model than the hyperbolic one, it presents an increase behavior at the future as is shown in the statefinder phase-space.

Finally, we analyze the SF diagnostic to distinguish the viscous models behaviour from the LCDM model one. In the $\{s, r\}$ -SF diagram the LCDM model is a fixed point located at $\{s, r\} = (0, 1)$. Figure 6 displays the $\{s, r\}$ -SF space of the models in the redshift interval $-1 < z < 2.5$. The arrows over the trajectories of the models show the evolution direction and the solid squares are the current position ($z = 0$) in the $\{s, r\}$ -SF plane. We observe that the viscous models have their evolution from the

quintessence region to LCDM model. However, the polynomial model has a increasing behaviour in the future with $\{s, r\}$ -point $(-4.3, 72.8)$ at $z = -1$ (see inner plot of Fig. 6), and for the tanh and cosh models end their evolution in the LCDM point.

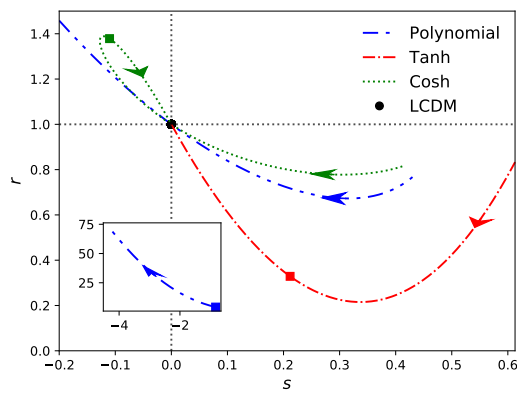


FIG. 6: $\{s, r\}$ -statefinder diagram using the best fit values of the joint analysis in the redshift region $-1 < z < 2.5$. The LCDM model is represented by a black solid circle at $(0,1)$. In blue double dot-dashed line is the trajectory of the polynomial model, and in red dash-dotted (green dotted) line is the trajectory of the tanh (cosh) model. The blue and red (green) solid square markers over the trajectories represent the position at $z = 0$. The arrows over the trajectories of the models mean the direction to the future.

V. CONCLUSIONS

The present work is devoted to study the Universe dynamics when a bulk viscosity is considered. We analyse three phenomenological models for the viscous bulk that are introduced in the Einstein equations as an effective pressure. Then we perform a Bayesian MCMC analysis to constraint the free parameters of the models using the latest sample of OHD and SNIa. The simplest one consists of a redshift polynomial function introduced by [44]. A form more complex was proposed by [48] that consist to model the bulk viscosity as tanh behaviour. We propose a phenomenological alternative to this model as a cosh form. We observe well agreement to the data but these three models have different behavior with respect to LCDM model when they are seen in the $\{s, r\}$ -statefinder space. We observe that they have a behaviour in the quintessence region. Also, the jerk parameter confirms a dynamical EoS of the three models. when we compare statistically these models, a Universe filled by non-perfect fluid is equally preferred by the observational data used over LCDM. Although we have a similar preference between viscous fluids, we observe that the hyperbolic models finish to the LCDM behaviour in the future. Finally, this kind of phenomenological viscous fluids studied is an interesting proposal to understand the dark sector in the context of the unified dark fluid.

ACKNOWLEDGEMENTS

The author thanks M. García-Aspeitia and J. Magaña for useful discussions to improve the manuscript. The author also thanks SNI Conacyt and Instituto Avanzado de Cosmología (IAC) collaborations. The author thankfully acknowledges computer resources, technical advise and support provided by Laboratorio de Matemática Aplicada y Cómputo de Alto Rendimiento del CINVESTAV-IPN (ABACUS), Proyecto CONACYT-EDOMEX-2011-C01-165873.

-
- [1] A. G. Riess, A. V. Filippenko, P. Challis, A. Clocchiatti, A. Diercks, *et al.*, The Astronomical Journal **116**, 1009 (1998).
 - [2] S. Perlmutter, G. Aldering, G. Goldhaber, R. A. Knop, P. Nugent, others, and T. S. C. Project, The Astrophysical Journal **517**, 565 (1999).
 - [3] T. M. C. Abbott and *et. al.*,
 - [4] Planck Collaboration, Ade, P. A. R., and *et. al.*, A&A **594**, A13 (2016).
 - [5] Planck Collaboration, Ade, P. A. R., and *et. al.*, A&A **594**, A14 (2016).
 - [6] S. Alam *et al.* (BOSS), Mon. Not. Roy. Astron. Soc. **470**, 2617 (2017), arXiv:1607.03155.
 - [7] M. Persic, P. Salucci, and F. Stel, Monthly Notices of the Royal Astronomical Society **281**, 27 (1996).
 - [8] A. Borriello and P. Salucci, Monthly Notices of the Royal Astronomical Society **323**, 285 (2001).
 - [9] C. S. Frenk, A. E. Evrard, S. D. M. White, and F. J. Summers, The Astrophysical Journal **472**, 460 (1996).
 - [10] J. Preskill, M. B. Wise, and F. Wilczek, Physics Letters B **120**, 127 (1983).
 - [11] L. D. Duffy and K. van Bibber, New Journal of Physics **11**, 105008 (2009).
 - [12] T. Matos, F. S. Guzmán, and D. Núñez, Phys. Rev. D **62**, 061301 (2000).
 - [13] L. A. Ureña López and T. Matos, Phys. Rev. D **62**, 081302 (2000).

- [14] T. Matos and F. S. Guzman, *Class. Quant. Grav.* **18**, 5055 (2001).
- [15] M. Rodríguez-Meza, *Advances in Astronomy* **2012**, 1 (2012).
- [16] M. A. Rodríguez-Meza, *AIP Conference Proceedings* **1473**, 74 (2012).
- [17] M. A. Rodríguez-Meza and J. L. Cervantes-Cota, *Mon. Not. R. Astron. Soc.* **350**, 671 (2004).
- [18] R. Catena and L. Covi, *The European Physical Journal C* **74**, 2703 (2014).
- [19] W. Hu and D. J. Eisenstein, *Phys. Rev. D* **59**, 083509 (1999).
- [20] M. Kunz, *Phys. Rev. D* **80**, 123001 (2009).
- [21] S. Chaplygin, *Sci. Mem. Mosc. Univ. Math. Phys* **21** (1904).
- [22] A. Yu. Kamenshchik, U. Moschella, and V. Pasquier, *Phys. Lett. B* **511**, 265 (2001), arXiv:gr-qc/0103004 [gr-qc].
- [23] N. Bilic, G. B. Tupper, and R. D. Viollier, *Phys. Lett. B* **535**, 17 (2002), arXiv:astro-ph/0111325 [astro-ph].
- [24] J. C. Fabris, S. V. B. Goncalves, and P. E. de Souza, *Gen. Rel. Grav.* **34**, 53 (2002), arXiv:gr-qc/0103083 [gr-qc].
- [25] J. Lu, *Physics Letters B* **680**, 404 (2009).
- [26] P.-H. Chavanis, *Physics Letters B* **758**, 59 (2016).
- [27] H. Hova and H. Yang, *International Journal of Modern Physics D* **26**, 1750178 (2017).
- [28] Hernández-Almada, A., Magaña, Juan, García-Aspeitia, Miguel A., and Motta, V., *Eur. Phys. J. C* **79**, 12 (2019), arXiv:1805.07895.
- [29] W. Zimdahl, *Phys. Rev. D* **53**, 5483 (1996).
- [30] A. A. Coley, R. J. van den Hoogen, and R. Maartens, *Phys. Rev. D* **54**, 1393 (1996).
- [31] S. Weinberg, *Rev. Mod. Phys.* **61**, 1 (1989).
- [32] I. Zlatev, L. Wang, and P. J. Steinhardt, *Phys. Rev. Lett.* **82**, 896 (1999).
- [33] R. R. Caldwell, M. Kamionkowski, and N. N. Weinberg, *Phys. Rev. Lett.* **91**, 071301 (2003).
- [34] M. Xin-He, R. Jie, and H. Ming-Guang, *Communications in Theoretical Physics* **47**, 379 (2007).
- [35] C. Eckart, *Phys. Rev.* **58**, 919 (1940).
- [36] W. Israel and J. Stewart, *Annals of Physics* **118**, 341 (1979).
- [37] L. P. Chimento, A. S. Jakubi, V. Méndez, and R. Maartens, *Classical and Quantum Gravity* **14**, 3363 (1997).
- [38] M. Cruz, N. Cruz, and S. Lepe, *Phys. Rev. D* **96**, 124020 (2017).
- [39] N. Cruz, E. González, S. Lepe, and D. S.-C. Gómez, *Journal of Cosmology and Astroparticle Physics* **2018**, 017 (2018).
- [40] G. P. Norman Cruz, Esteban Gonzalez, (2018), arXiv:1812.05009 [astro-ph].
- [41] M. M. Disconzi, T. W. Kephart, and R. J. Scherrer, *Phys. Rev. D* **91**, 043532 (2015).
- [42] G. L. Murphy, *Phys. Rev. D* **8**, 4231 (1973).
- [43] V. A. Belinskii and M. Khalatnikov, *Zh. Eksp. Teor. Fiz.* **69**, 401 (1975).
- [44] M. Xin-He and D. Xu, *Communications in Theoretical Physics* **52**, 377 (2009).
- [45] J. Magana, M. H. Amante, M. A. Garcia-Aspeitia, and V. Motta, *Monthly Notices of the Royal Astronomical Society* **476**, 1036 (2018), arXiv:1706.09848.
- [46] D. M. Scolnic and *et. al.*, *The Astrophysical Journal* **859**, 101 (2018).
- [47] I. Brevik and O. Gorbunova, *General Relativity and Gravitation* **37**, 2039 (2005).
- [48] V. Folomeev and V. Gurovich, *Physics Letters B* **661**, 75 (2008).
- [49] V. Sahni, T. D. Saini, A. A. Starobinsky, and U. Alam, *Journal of Experimental and Theoretical Physics Letters* **77**, 201 (2003).
- [50] U. Alam, V. Sahni, T. Deep Saini, and A. A. Starobinsky, *Monthly Notices of the Royal Astronomical Society* **344**, 1057 (2003).
- [51] A. Al Mamon and K. Bamba, (2018), arXiv:1805.02854 [astro-ph.CO].
- [52] D. Foreman-Mackey, D. W. Hogg, D. Lang, and J. Goodman, *pasp* **125**, 306 (2013), arXiv:1202.3665 [astro-ph.IM].
- [53] A. Gelman and D. Rubin, *Statistical Science* **67**, 457 (1992).
- [54] R. Jimenez and A. Loeb, *Astrophys. J.* **573**, 37 (2002), arXiv:astro-ph/0106145 [astro-ph].
- [55] E. Komatsu *et al.* (WMAP), *Astrophys. J. Suppl.* **192**, 18 (2011).
- [56] H. Akaike, *IEEE Transactions on Automatic Control* **19**, 716 (1974).
- [57] N. Sugiura, *Communications in Statistics - Theory and Methods* **7**, 13 (1978), <https://doi.org/10.1080/03610927808827599>.
- [58] G. Schwarz, *Ann. Statist.* **6**, 461 (1978).
- [59] A. R. Liddle, *Monthly Notices of the Royal Astronomical Society: Letters* **377**, L74 (2007), <http://oup.prod.sis.lan/mnrasl/article-pdf/377/1/L74/4044139/377-1-L74.pdf>.
- [60] Z. Davari, M. Malekjani, and M. Artymowski, *Phys. Rev. D* **97**, 123525 (2018).